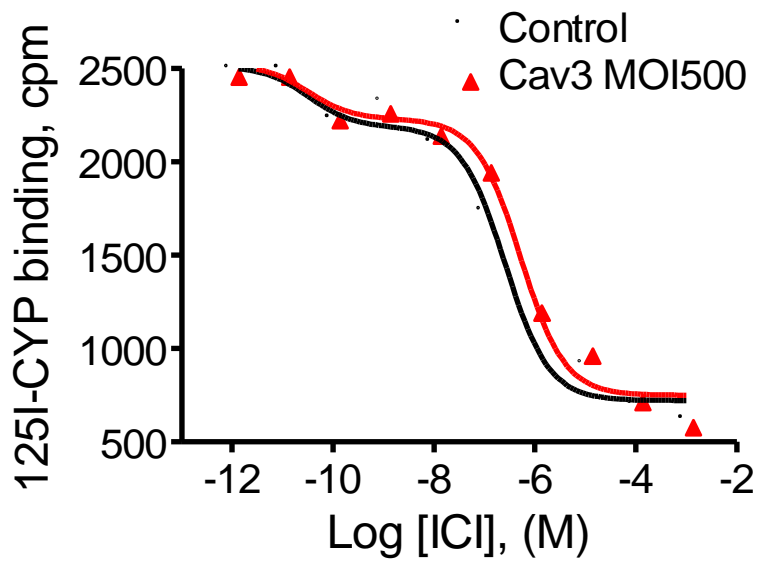
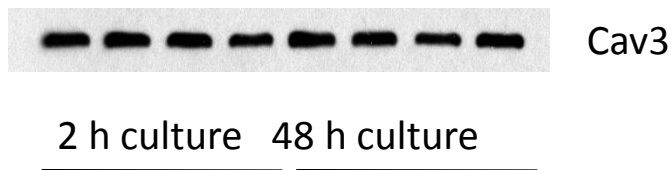


# Supplementary Figure 1

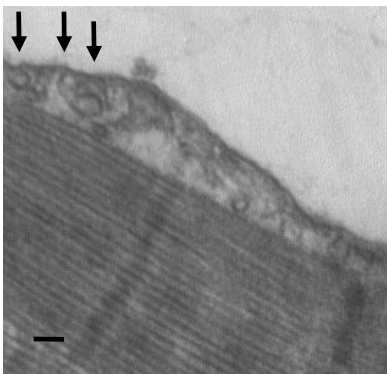
**A**



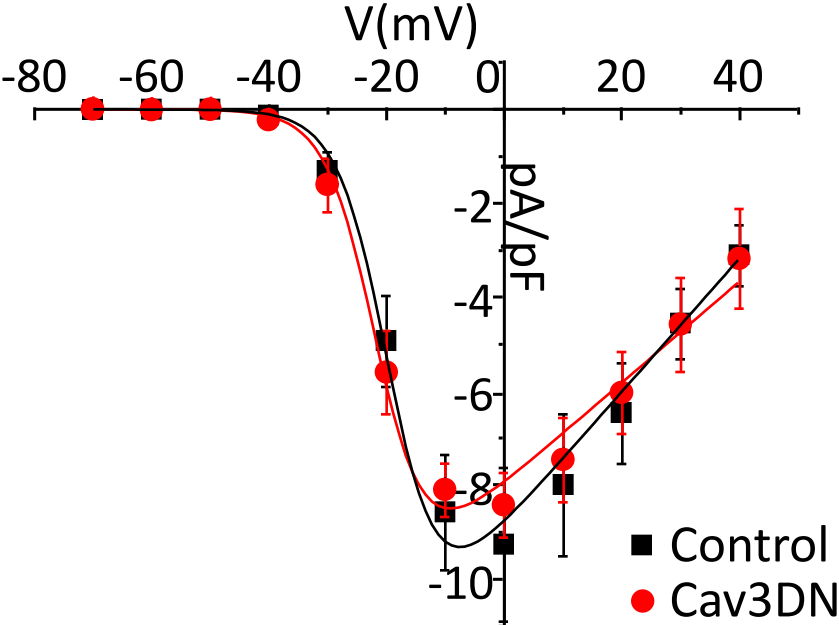
**B**



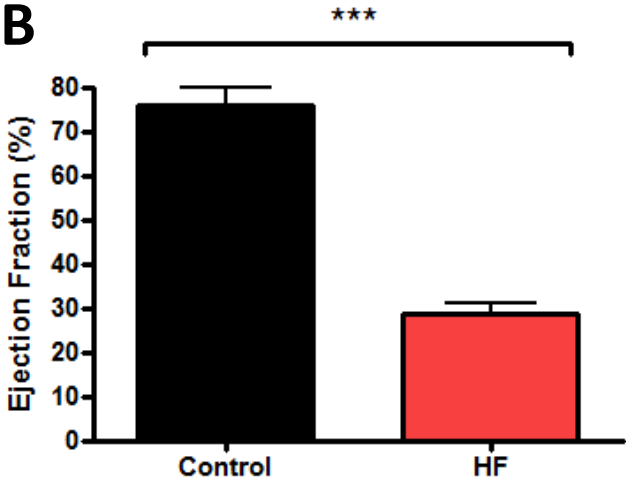
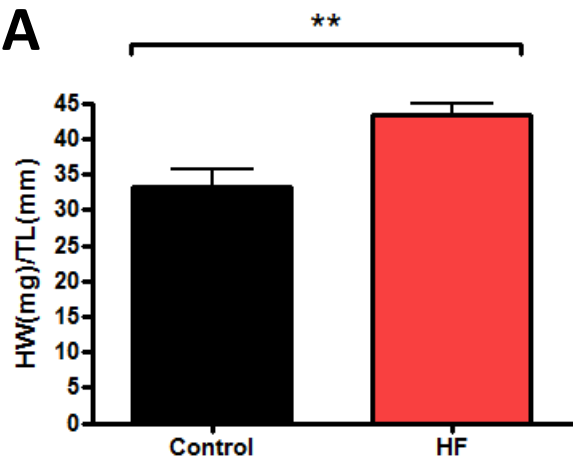
**C**



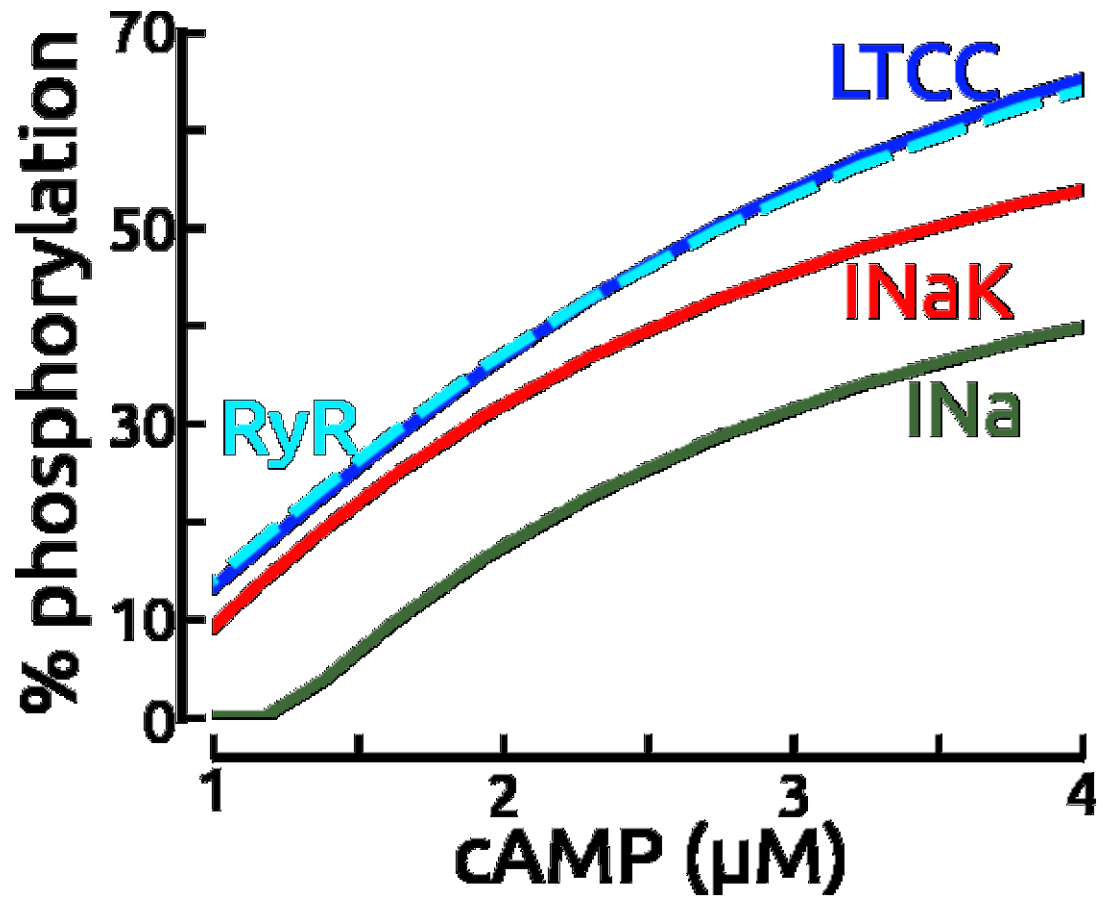
# Supplementary Figure 2



# Supplementary Figure 3



Supplementary Figure 4



### Supplementary Figure 1

Cav3 overexpression does not affect the number and proportion of  $\beta_1$  or  $\beta_2$ ARs in ARVMs.

- A)** Radioligand binding studies to compare  $\beta_1$  and  $\beta_2$ AR densities were performed in membranes isolated from ARVMs 48h after infection with either LacZ or Cav3 adenovirus (both at MOI 500). Representative displacement curves for ICI118551 are shown (n=3). The first fraction of the displaced radioligand corresponds to  $\beta_2$ AR, the second fraction – to  $\beta_1$ AR.
- B)** *Culturing does not alter Cav3 expression so all effects are due to Cav3 or Cav3DN overexpression.*
- C)** Caveolae numbers are not altered by culture, as demonstrated by the electron micrograph shown.

### Supplementary Figure 2

Cav3DN (MOI 500) in isolated adult cardiac myocytes does not affect the density of the L-type  $\text{Ca}^{2+}$  current recorded in whole cell patch clamp experiments.  $V_{0.5\text{act}}$  values were:  $-17.96 \pm 1.69\text{mV}$  in control (LacZ) vs.  $-19.96 \pm 1.49\text{mV}$  in Cav3DN expressing cells (means  $\pm$  SE, n=7).

### Supplementary Figure 3

Biometric and echocardiographic data obtained from rats with chronic HF model.

- (A) Hearts were significantly hypertrophied as indicated by elevated heart weight/tibia length ratio (n=6 in each group). \*\*p<0.01
- (B) Ejection fraction was significantly reduced confirming impaired systolic function in these rats (n=6 in each group). \*\*\*p<0.001

#### **Supplementary Figure 4**

Percentage of membrane targets that are phosphorylated by PKA (y-axis) is sensitive to cAMP clamp to values ranging 1 to 4  $\mu\text{M}$  (x-axis). This shows that cAMP values in this range, as seen in **Figure 6** simulations, are physiologically relevant. Targets shown include: L-type Ca channel (LTCC, blue), ryanodine receptor (RyR, cyan), Na/K-ATPase (INaK, red; effect mediated by phospholemman interaction) and fast Na current (INa, green). This assumption was generated from the Heijman model [39] exploring the effects of  $\beta\text{AR}$  stimulation upon downstream effectors.

## **Supplementary Text**

*The computer model used in the current study borrows heavily and directly from the recent work of Heijman et al. 2011 [1]. Aspects of the Heijman et al. model that are important for understanding behaviours simulated here are summarized below for convenient reference. For detailed information regarding other components and feedbacks not summarized here, refer to the original Heijman publication and its extensive supplemental materials.*

*Heijman et al. represented the  $\beta$ -adrenergic signaling cascade, which relates  $\beta$ -agonist input, specified by isoproterenol (ISO) dose, to downstream outputs of percent phosphorylation of various targets by protein kinase A (PKA). Important events along the cascade include the following: 1) ISO binds to  $\beta$ -adrenergic receptors ( $\beta$ ARs, here we stimulate only type 2 receptors,  $\beta_2$ ARs). 2) G-proteins coupled to  $\beta$ ARs activate adenylyl cyclase. 3) Formation of cyclic adenosine monophosphate (cAMP) is catalyzed by adenylyl cyclase. 4) cAMP activates PKA, which phosphorylates targets. 5) cAMP is decomposed by phosphodiesterases (PDEs).*

*These processes are played out in three diffusion-coupled but separate compartments referred to as signaling domains. They include the bulk cytosol (cyt), the membrane associated caveolae (cav), and and extra-caveolae (ecav) domains. The volume of the cyt domain is about 70%, while cav and ecav comprise 2 and 4% of the total cell volume, respectively.*

*The FRET sensor used in experiments in the present study measured bulk cytosolic cAMP. Simulations shown in this study plot cAMP at the membrane, where the majority of important PKA targets are membrane associated (e.g. L-type Ca channel, ryanodine receptors, and Na channels). Our model predicts that cAMP in the cytosol (cyt) is a mirror for membrane cAMP. This was not surprising given that the cyt domain is passive, lacking  $\beta_2$ ARs. However, cAMP concentrations were ~ten-*

*fold lower in the cytosol; we account for this by the fact that cyt volume is ~ten-fold larger than the sub-membrane volume.*

*Domains cav and ecav include distinct PDE activity levels. In the small volume of the cav domain, cAMP is tightly regulated by relatively high activity of PDE types 2, 3 and 4. Regulation is relatively weakly controlled in ecav, where the volume is twice as large and where PDE type 3 is absent; both tend to reduce cAMP decomposition. This leads to higher cAMP in ecav than in cav under basal conditions and in response to ISO.*

*Supplemental materials in the paper by Heijman et al. describe the decision process used to determine parameters (see Heijman et al. Supplement Figure S1 for a description). In brief, parameters defined by data from the literature were set as measured, and others were defined using global behavioural data (e.g. rate of action potential changes in response to ISO, rate of L-type Ca channel phosphorylation) and conceptual constraints. Sensitivity to perturbations in parameters was examined to determine critical role players in various outputs and also to demonstrate overall model stability and robustness (see Heijman et al. Supplement Figures S28-S30).*

*Augmentation of the Heijman model implemented in order to simulate diffusion over the long axis of the ventricular myocyte is described in the manuscript Methods section 2.9. Integration was performed using Matlab (The Mathworks, versions R2012a and R2013a, Natick, MA).*

[1] Heijman J, Volders PGA, Westra RL, Rudy Y. Local control of  $\beta$ -adrenergic stimulation: Effects on ventricular myocyte electrophysiology and Ca(2+)-transient. *Journal of Molecular and Cellular Cardiology* 2011;50:863